Available online at www.sciencedirect.com
ScienceDirect
Carbohydrate Polymers 68 (2007) 249–259
Carbohydrate Polymers
www.elsevier.com/locate/carbpol

Starch in rubbery and glassy states by FTIR spectroscopy

Isabelle Capron [a,*], Paul Robert [a], Paul Colonna [a], Maurice Brogly [b], Véronique Planchot [a]

[a] INRA, Unité de Recherche Biopolymères, Interactions et Assemblages – rue de la géraudière, BP 71 627 – 44316 Nantes Cedex 3, France
[b] CNRS, Institut de Chimie des Surfaces et Interfaces, 15 rue Jean Starcky, 68057 Mulhouse, France

Received 31 August 2006; received in revised form 8 December 2006; accepted 12 December 2006
Available online 23 December 2006

Abstract

The organization of various starch samples varying in molecular structure, organization and moisture content was studied by ATR-FTIR spectroscopy. The comparison of the infrared spectra showed that band intensities in the 1065–870 cm^{-1} region can be explained by their mobility related to the glass transition, T_g, which occurs at room temperature in the 15–21% water content range. Spectra analyzed using principal component analysis showed main structure/moisture changes for the 1000/1022 cm^{-1} intensity ratio. The helix organization at a short order range was weakly moisture dependant below T_g, whereas the signal became increasingly water dependant with the crystalline/amorphous ratio above T_g. This result is in agreement with the model of liquid crystal structure and mesophase variation: water allows the self-assembly of amylopectin helices leading to layered organized structure.

Keywords: Infrared; Structure; Controlled moisture; Liquid crystal model; Phase transition; Biopolymers

1. Introduction

Starch is one of the most studied biopolymers (Buléon, Colonna, Planchot, & Ball, 1998; French, 1984; Guilbot & Mercier, 1985; Oostergetel & van Bruggen, 1993). However, some structural aspects involving the arrangement of the molecules inside native starch granules and starchy materials are still matter of debate. Starch granules can be considered as a combination of two components, amylose and amylopectin. They both consist of α(1–4) linked D-glucose units. Amylose is essentially linear, whereas amylopectin is a highly branched polymer due to 5–6% of α(1–6) links (Buléon et al., 1998). The native structure of starch is made of helices that are more or less radially organized forming a granule, which has to be described at different length scales. The internal architecture of native starch granules is characterized by concentric rings representing semi-crystalline shells (thickness 120–400 nm) separated by essentially amorphous regions. There is much evidence that the semi-crystalline shells consist of regular alternating amorphous and crystalline lamellae repeating at 9–10 nm (Cameron & Donald, 1993). In this structural organization, parallel double helices of amylopectin side chains are assembled into radially oriented clusters (Fig. 1). The X-ray scattering study of crystallites showed that helices are organized according to two main crystalline lattices: an A-type allomorph mainly found in cereal starches and a B-type allomorph found in tubers and amylose-rich starches. A C-type structure is known as a mixed organization of A and B crystalline forms (Buléon, Gérard, Riekel, Vuong, & Chanzy, 1998).

More recently, the organization of the semi-crystalline shells in the 9–10 nm lamellae has been described as a chiral side-chain liquid crystalline polymer (SCLCP) by Donald and co-workers (Daniels & Donald, 2004; Waigh et al., 2000). According to that assumption, amylopectin in the granule is modeled as a three components system including (i) a flexible backbone, (ii) mesogen units analyzed as rigid double helices blocs and (iii) short chains called flexible spacers, localized between the mesogen units and the backbone. These spacers tend to limit the coupling of the helices motion to that of the backbone. On this basis, the process involved during hydration of dry starch can be interpreted

* Corresponding author. Tel.: +33 2 40 67 50 95; fax: +33 2 40 67 51 67.
E-mail address: capron@nantes.inra.fr (I. Capron).

0144-8617/$ - see front matter © 2006 Elsevier Ltd. All rights reserved.
doi:10.1016/j.carbpol.2006.12.015

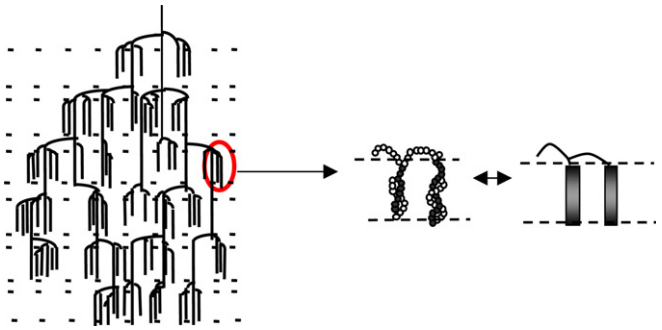

Fig. 1. Schematic representation of an amylopectin molecule. Left: global view. Middle: a zoom on side-chains organization in a semi-crystalline phase. Clusters are made of aligned double helices. Right: mesogen units linked by spacers in the liquid crystal model (according to Daniels and Donald, 2004).

as a mesophase change from glassy state driving to a nematic structure (Fig. 2a), to an hydrated lamellar smectic structure induced by the enhanced mobility of the flexible backbone and spacers (Fig. 2b). This model commonly accepted is supported by results from small and large-angle X-ray scattering. However, no use of infrared has been presented in the literature to support this model, in contrast to other polymer dispersed liquid crystal films (McKenna, Miller, & Peterson, 2004).

The infrared spectroscopy, considering interactions at a local range order, has already been used to describe the organization and structure of starch at various water contents. Previous works on gelatinization and retrogradation of starch have proved the efficiency of infrared spectroscopy to study conformational changes (Bernazzani, Chapados, & Delmas, 2000; Cael, Koenig, & Blackwell, 1973; Goodfellow & Wilson, 1990; Liu, Charlet, Yelle, & Arul, 2002; Wilson, Kalichevsky, Ring, & Belton, 1987). While amorphous starch was characterized by an absorbance band around 1022 cm^{-1}, the crystalline state could be identified by the development of a band at 1047 cm^{-1} (van Soest, Tournois, de Wit, & Vliegenthart, 1995). More precisely, the absorbance band at 1047 cm^{-1} is composed of two overlapping bands at 1040 and 1053 cm^{-1}. During retrogradation, 1040 cm^{-1} and the formation of helices develop within several hours, whereas 1053 cm^{-1} increases over longer periods with aggregation and crystallization of starch molecules (Goodfellow & Wilson, 1990). In the 1300–800 cm^{-1} region, the C–C, C–O, C–H stretching and COH bending modes are observed (Cael, Koenig, & Blackwell, 1975) and below 800 cm^{-1} appear the skeletal and ring modes (Vasco, Blackwell, & Koenig, 1972). Vibrational spectra of glucosyl monomers, oligomers and polymers in solution and solid state are rather similar, indicating that observed frequencies arise from similar modes (Vasco, Blackwell, & Koenig, 1971). Most of the previous structural studies using FTIR were performed in highly hydrated conditions (>60% water w/w db) (Goodfellow & Wilson, 1990; Liu et al., 2002; Wilson et al., 1987; Sevenou, Hill, Farhat, & Mitchell, 2002) or non completely described sample conditions (Cael et al., 1973; Liu, Himmelsbach, & Barton, 2004). Only few studies are based on powdered starch samples with controlled water contents. While van Soest et al. (1995) compared samples heated up to 195 °C containing 10–50% water (w/w db), Bernazzani et al. (2000) submitted a sample containing 30% water (w/w db) to cycles of temperature up to 120 °C.

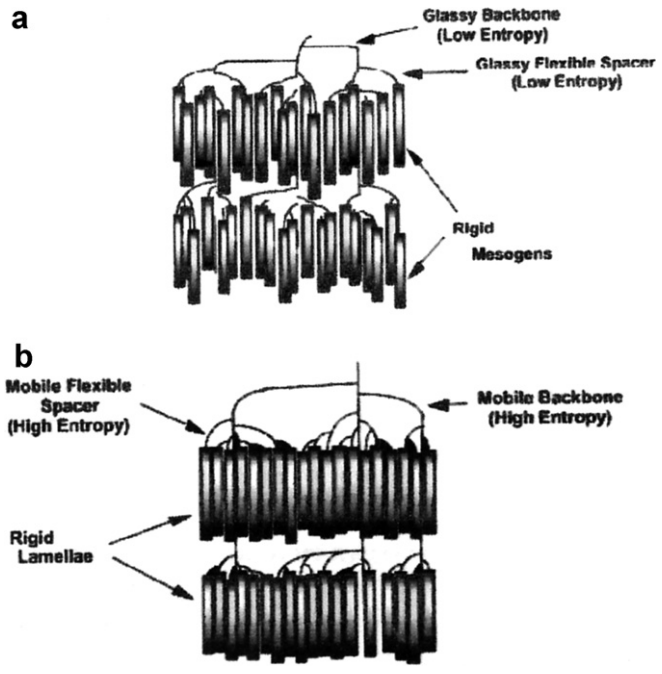

Fig. 2. Representation of the process involved in amylopectin clusters during hydration on a crystalline lamellar structure according to the smectic side-chain liquid crystalline polymer model. (a) Dry starch in a glassy nematic state, (b) hydrated starch with flexible spacers and backbone forms a smectic lamellar structure. (Reprinted from Daniels and Donald, 2004.)

Actually most of the authors have used infrared spectroscopy to estimate the amount of ordered or crystalline domains by evaluating the absorbance intensities at 1047 and 1022 cm^{-1}. The signal around 1000 cm^{-1} was unclearly recognized as water sensitive and related to intramolecular hydrogen bonding of hydroxyl groups (van Soest et al., 1995) or plasticizing effect of water (Kacurakova & Mathlouthi, 1996). All authors agree to notice that it is not possible to assign the bands individually, given that each band is linked to another as a result of highly coupled vibrational modes, which create differences in assignment. These discrepancies evidenced a need of new studies for a better use of these bands.

It is accepted that amorphous parts of starch undergo a transition from glassy to rubbery state. This can be induced either by increasing the temperature (Bizot et al., 1997) or by enhancing the water content (Slade & Levine, 1993). Taking this transition commonly called glass transition, T_g, into account could change the way of interpreting these results. Below the glass transition, the segmental mobility of polymer chains is frozen in a random conformation, making all starch phases solid and glassy. When the temperature or the water content increases, a molecular motion is initiated, enabling molecule segments to slide one over another.

This physical event reflects the increase in the motion of short segments (3–20 monomers). Above the T_g the material becomes rubber-like (mobile): structural transformations are allowed in the amorphous zones. Water exerts a plasticizing effect on the amorphous zones where its influence on ordered zones is not explained. Only a few IR papers deal with the glass transition process (Czarnik-Matusewicz, Pajak, & Rospenk, 2005; D'Ilario, Lucarini, Martellini, & Piozzi, 1997) although clear results can be obtained by this technique. Recent works have shown that infrared can be used to monitor the length and the strength of intermolecular hydrogen bonds in sugar glasses. Wolkers, Oliver, Tablin, and Crowe (2004) found a positive correlation between ν_{OH} connected to the length of the hydrogen bonds and the glass transition temperature. With poly(vinylpyrrolidone), a spectroscopic investigation for the presence of interactions between the drugs and PVP proved to be extremely predictive of the plasticizing effect of a large range of molecules (Nair, Nyamweya, Gonen, Martinez-Miranda, & Haog, 2001).

The aim of the present paper is to study the variation observed on Fourier transform infrared (FTIR) spectra obtained using attenuated total reflectance (ATR) device to powders of starch materials at various controlled hydrations. This variation in water content below and above the threshold of 15–21% w/w db allowed to compare the samples in rubbery and glassy states at room temperature.

2. Materials and methods

2.1. Materials

Potato and maize starches were a gift from Roquette Frères (Lestrem, France). Glycogen was purchased from Fluka (Sigma, France) and manioc starch was extracted in our laboratory.

Starch samples varying in their botanical origin, amorphous/crystalline ratio, crystalline type (A, B or C) and composition (Table 1) were selected.

- Glycogen and extruded potato (Della Valle, Boche, Colonna, & Vergnes, 1995) were chosen as amorphous references.
- Native granular starches from potato, manioc and maize (waxy, normal and high-amylose maize) were chosen as semi-crystalline samples.
- Crystalline residues (lintners) prepared from mild acid hydrolysis (Robin, Mercier, Duprat, Charbonnière, & Guilbot, 1975) were obtained from potato, manioc, normal maize and high amylose maize granular starches.

Table 1
Samples used

Starch	Type	Diameter (μm)	% amylose[a]	Crystalline type starch/ lintner	% crystalinity[b] starch/ lintner
Potato	Tuber	5–100	20	B/B	47/53
Manioc	Root	4–35	17	A/C	44/73
Waxy maize	Cereal	5–30	<1	A/A	46/76
Normal maize	Cereal	5–30	25	A/C	34/53
High amylose maize	Cereal	5–30	70	B/B	31/61

[a] cf. Buléon et al. (1998).
[b] X-ray determination (Planchot, 1993).

2.2. Samples preparation

Annealed sample was obtained by heating an aqueous dispersion of native potato starch (30% by weight on a dry starch basis including 0.02% NaN_3) at 50 °C for 24 h. After centrifugation, the residue was washed with distilled water and dried at 40 °C in an oven overnight.

Grinded samples were obtained from native potato and high-amylose maize granular starches by mechanical breakage using a cryo-grinder (freeze/mill, Spex, USA). About 2 g of starch powder were deposited in tubes including a metallic pestle, immerged in liquid nitrogen and grinded by magnetic action of the pestle during 5 cycles of 2 min to avoid any gelatinization phenomena.

All samples were conditioned at various humidities at 20 °C for three weeks using desiccators under vacuum with saturated salt solutions. Seven different salts (P_2O_5; K_2CO_3; NaBr; $SrCl_2$; NaCl; KCl and $BaCl_2$) were used for seven water activities (0; 0.43; 0.58; 0.71; 0.75; 0.84 and 0.90, respectively). The water content was determined for each sample (2 h at 130 °C) and always expressed as water/starch on dry basis.

2.3. DSC measurements

The temperature of starch gelatinization of native and annealed granular potato starches was measured by differential scanning calorimetry (DSC Q100 TA Instruments) to confirm effective annealing of the potato starch sample. The samples were deposited in excess water (about 80%) in stainless steel pan (100 μl; 30 bars) hermetically sealed and heated from 5 to 153 °C with a heating rate of 3 °C/min.

2.4. Granulometric measurements

The size variation of the granules was determined (Micrometrics Int. Co Saturn Digiziser 5200 V1-08) using the Mie scattering theory. The refractive indices were 1.53 for the starch granules and 1.33 for the solvent, and the absorption index was 0.1 (Nayouf, Loisel, & Doublier, 2003).

2.5. FTIR measurements

Infrared spectra were recorded on two different spectrometers: the IFS 66/S (Bruker, Wissembourg, France)

and the IR 550 Magma (Nicolet, Billerica, USA). Both systems were equipped with a Golden gate attenuated total reflectance (ATR) accessory with a diamond crystal in monoreflexion at an angle of incidence of 45°. Samples conditioned in relative humidity were measured directly after pressing the sample onto the crystal. Recording a second spectrum 5 min after having collected the first one allowed to check that no drying effect interfered during measurement. The spectra, obtained at a resolution of 2 cm^{-1}, were averages of 100 scans and recorded against an empty cell as background.

In ATR mode, the IR beam passes through the diamond crystal and reflects totally when $\theta i > n_2/n_1$ with θi the angle of incidence, n_1 and n_2 the refractive indices of the crystal and the sample. The intensity of absorption depends on two main parameters: a good contact of the sample with the crystal and the depth of penetration in the sample expressed as (Harrick, 1979)

$$d_p = \frac{\lambda}{2\pi n_1 \sqrt{\sin^2 \vartheta_i - \left(\frac{n_2}{n_1}\right)^2}}$$

where λ is the wavelength of the incident wave, θ_i the incident wave angle (45° for diamond), $n_1$and n_2 the refractive indices of the crystal and the sample (2.4 and 1.53, respectively). In the wavelength range considered (1065–870 cm^{-1}) the average penetration depth is about 2 μm.

The glass to rubber transition is known to be time dependent. Various starch samples (potato, high amylose maize, normal maize and waxy maize) were measured after a stabilization of 3 weeks and also after 3 months. For all tested samples the spectra superimposed nicely, which means that kinetics effects on the spectra are negligible compared to the observed structure and to the water content variations.

All spectra were cut and baseline corrected by drawing a straight line between 1065 and 875 cm^{-1} using Grams 32 software (Galactic Inc., Waltham, USA). The spectra were normalized and compared to each other.

2.6. Principal component analysis

The FTIR spectra recorded in the wavelength range 1065–870 cm^{-1} from powdered products at the seven hydration states were analyzed by applying principal component analysis (PCA). PCA is a multivariate data treatment which reveals the similarities within the spectra by taking all the wavenumbers into account. Similarity maps, drawn from the principal component scores, are used to compare samples with each other and to define clusters. The spectral patterns provide information about the characteristic absorption bands which explain the similarities of the samples observed on the maps (Robert, Devaux, & Bertrand, 1996). The computation of principal components is based on the diagonalisation of the variance–covariance matrix

$$\mathbf{V} = \mathbf{X}'\mathbf{X}$$

assessed from the centered spectral data $\mathbf{X}_{n,v}$ (n, samples; v, wavenumbers). Diagonalisation achieves the decomposition of $\mathbf{V}$ into eigenvectors $\mathbf{L}$ and eigenvalues $\mathbf{S}$. The eigenvectors, often called loadings, are used to assess the principal component scores $\mathbf{C}$

$$\mathbf{C} = \mathbf{XL}$$

The eigenvalues indicate the percentage of total variance described by each principal component. Similarity maps of the samples are plotted from the scores of two given principal components. Spectral patterns derive from eigenvectors.

The absorbance values were analyzed with Statgraphics plus 5.1 and Uniwin plus 5.11 software (Sigma Plus, Levallois-Perret, France).

3. Results and discussion

A set of sample was chosen to evaluate the differences observed for a large panel of structures of starch material from amorphous to crystalline. Therefore, samples varying in crystalline type (A, B and C), amylose content (0–70%), composition and botanical origin have been selected. Their FTIR spectra have been compared at seven different water contents (0–29% w/w db).

3.1. FTIR spectra analysis

To illustrate structural differences, extruded, granular and lintner potato starch samples were first used to compare the amorphous, semi-crystalline and crystalline organizations respectively. The infrared spectra of the three samples in the highest hydrated conditions used (19.0–23.7% w/w db) are given on Fig. 3. While the lintner and granular starch samples were characterized by a major absorption band at about 1000 cm^{-1}, the extruded sample revealed two peaks at 1000 and 1022 cm^{-1}. A small absorption band around 1047 cm^{-1} was depicted for the lintner and granular starch samples. The COH bending modes observed at 1047 and 1022 cm^{-1} have already been assigned to ordered and amorphous starch samples, respectively (Liu et al., 2002; Sevenou et al., 2002).

The water content of samples measured at given water activities showed a non linear behavior evidencing a structural influence on water sorption (French, 1984). A comparison of granular potato starch and potato-starch-derived samples (Fig. 4) indicated that lintners in the 0–17% (w/w db) water content range systematically retained less water than granular starch and amorphous sample. Above about 17% (w/w db) water content, lintners showed an enhanced affinity for water. This behavior was observed whatever the botanical origin of starch. Fig. 5 shows the hydration effect of lintners and extruded samples issued from potato starch on infrared spectra. Lintners at 22.3%

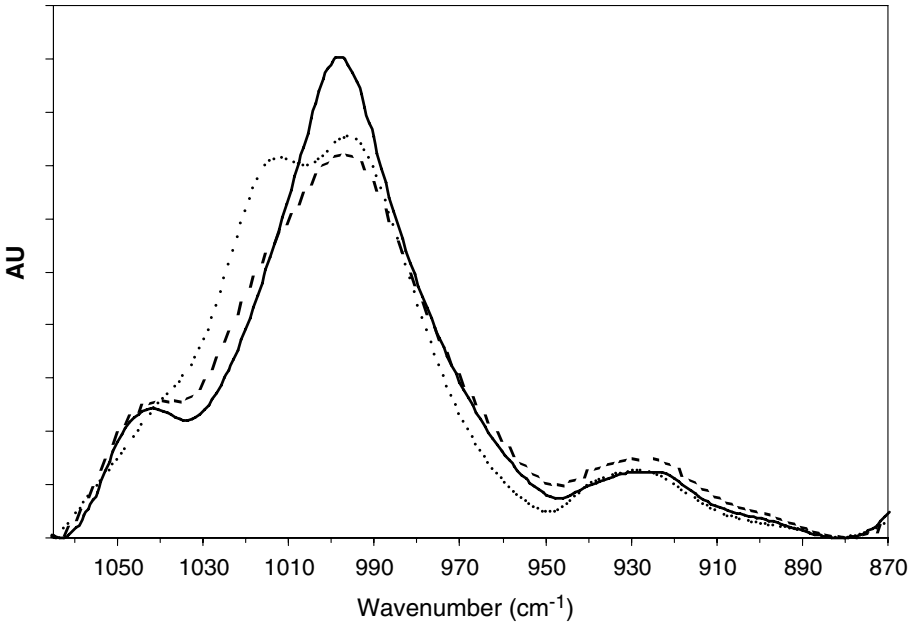

Fig. 3. FTIR spectra of three samples derived from potato starch varying in structure at highly hydrated conditions. Water content is given in bracket (w/w db) ··· extruded starch (19.7%); - - - - granular starch (23.7%); — lintner (22.3%).

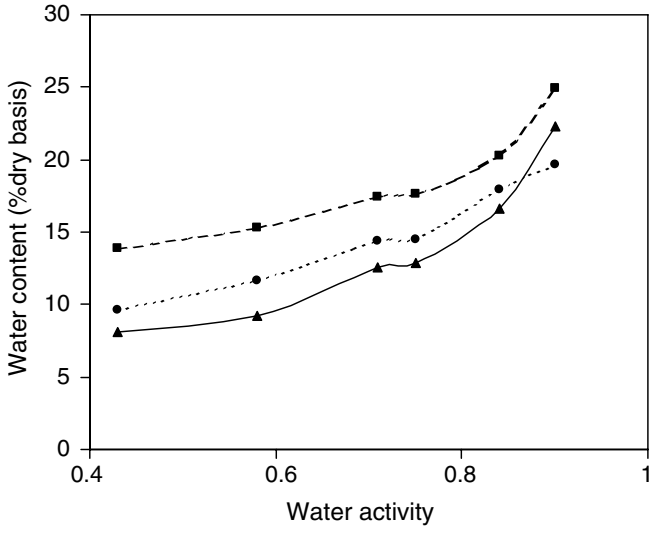

Fig. 4. Measured water content compared to the water activity of conditioning saturated salt solutions for the samples derived from potato starch. ● extruded starch; ■ Granular starch; ▲ Lintner.

water content were characterized by an intense absorption band at 1000 cm^{-1} and a shoulder at 1047 cm^{-1}.

For strictly anhydrous lintners, a decrease of the absorption intensity at 1000 cm^{-1} was accompanied by a broadening of the band towards high wavenumbers. This peak broadening at these low water contents was also observed by ^{13}C CP/MAS NMR and X-ray results (Guilbot & Mercier, 1985; Paris, Bizot, Emery, Buzaré, & Buléon, 1999). These results suggest that at low water contents, a wide distribution of molecular conformations and bond energies lead to the distortion of the crystal lattice.

In the particular case of the amorphous sample, broadening of infrared spectra appeared towards low wavenumbers (950–990 cm^{-1}) with decreasing water content. This spectral region was assigned to glycosidic bonds (Kacurakova & Mathlouthi, 1996). As no change was observed for lintners (crystalline samples) in this spectral range, the molecular changes involved should be initiated in amorphous domains.

The infrared spectra of samples issued from maize and manioc under granular and lintnerized forms and amorphous glycogen were recorded in the same conditions and compared at 7 water contents. They all revealed almost the same intensity changes with organization and humidity as previously described for potato.

The spectral region investigated, 1065–870 cm^{-1}, was assigned to C–O, C–C and C–H stretching modes in alcoholic COH moieties. Infrared absorbances generated from deformations of the various C–O–H valence angles are very sensitive to the degree of hydration (Cael et al., 1975). The best accepted model for α-glucan organization in amylopectin within the semi-crystalline part of the granules involves double helix structures linked to each others by chains (the spacers) to form clusters (see Fig. 1). As proposed by Imberty, Chanzy, Perez, Buléon, and Tran (1988), all hydrogen atoms are located inside the double helix, whereas hydroxyl groups are found outside. Upon moisturizing, new hydrogen bounds are formed with alcohols and water molecules localized in the unit cells (4 and 36 water molecules per unit cells in the A and B structures respectively) (Imberty, Buléon, Tran, & Perez, 1991). As proposed for cellulose (Maréchal & Chanzy, 2000), primary alcohols at C6 position may rotate around C5–C6 bond and adopt more stable conformations stabilized by

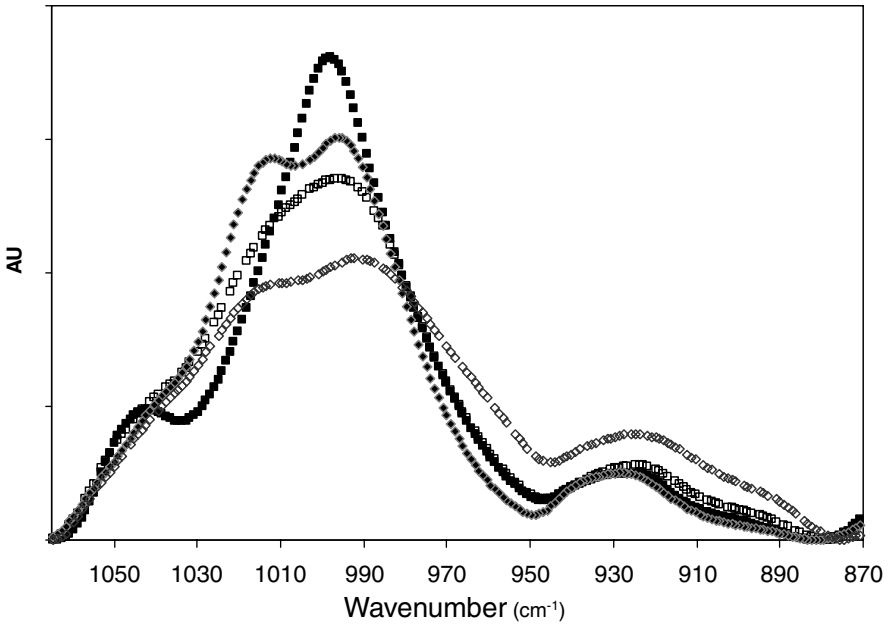

Fig. 5. Hydration effect on the FTIR spectra of extruded and lintnerized potato starch samples. Water content is given in bracket (w/w db). ■ lintner (22.3%); □ lintner (0%); ◆ extrudate (19.7%); ◇ extrudate (0%).

hydrogen bonds. van Soest et al. (1995), studying the influence of water content on starch samples, related the 1000 cm^{-1} infrared band to hydrogen bonding of the hydroxyl group at C6. As far as these links are located between the double helices, it could allow inter-double-helices links inducing significant modification in the global double helices associations. Favorable links should thereby result in a narrowing of the peaks as observed on the spectra for lintners (crystalline samples) with increasing water content (Fig. 5).

3.2. Principal component analysis

The large sample set and the high correlation between infrared absorption bands make the analysis difficult. Principal component analysis (PCA) applied to infrared spectra was, therefore, carried out on the 1065–870 cm^{-1} spectral region. A previous study by DSC measurements (Bizot et al., 1997), established that the calorimetric glass transition, T_g, can be controlled by managing the water content in the sample for various types of α-glucans at 20 °C. These authors showed that the glassy/rubbery transition occurs at 21% water content (w/w db) for phytoglycogen, and two destructured granular starches (potato and waxy maize). This value was taken as the water content at which the glass transition occurs for glycogen, extruded starch and all granular starches. The same transition was shown to shift to about 15% water (w/w db) for destructured potato lintners at 20 °C (Bizot et al., 1997). We conclude that at 20 °C, the glassy to rubbery transition occurs in the 15–21% water content range.

As no clear tendency could be established on the whole sample set, two separated principal component analyses were applied to the infrared spectra of samples, respectively, below and above the glass transition (i.e. 15 or 21% w/w db). Above the glass transition as samples are in a rubbery state, the similarity map defined by principal components 1 and 2 (96.6% of the total inertia) discriminated amorphous, semi crystalline and crystalline samples well (Fig. 6). For dryer samples, in the glassy state, the discrimination between crystalline and amorphous samples was less obvious (Fig. 7). The difference between the results obtained above and below the transition were interpreted using the side-chain liquid crystalline polymer model (SCLP) (Waigh et al., 2000). Upon water sorption, the molecule flexibility increased by new hydrogen bonds reorganized the rigid mesogenic units into layered structures (Fig. 2).

No interpretation on the meaning of the principal component 1 (53.0% of the total inertia) has been successful. In contrast, the spectral pattern derived from loadings of the principal component 2 (43.6% of the total inertia) made it possible to depict infrared spectral changes observed on samples above T_g (Fig. 8). The spectral pattern opposed 1000 and 1022 cm^{-1}, the absorption band at 1000 cm^{-1} being developed with hydrated crystalline samples and 1022 cm^{-1} with amorphous samples.

An interesting result is the low contribution of the absorption band at 1047 cm^{-1} – assigned to the helices formation – in PC1 and PC2 for the three families of samples: amorphous, semi-crystalline (granular starches) and crystalline (lintners). It shows the major effect of organization induced by hydration process on the spectra compared to structural differences. Indeed the comparison of samples inside each family cannot reveal this band, as the length of the double helices (i.e. mesogens) is stable when varying the hydration level.

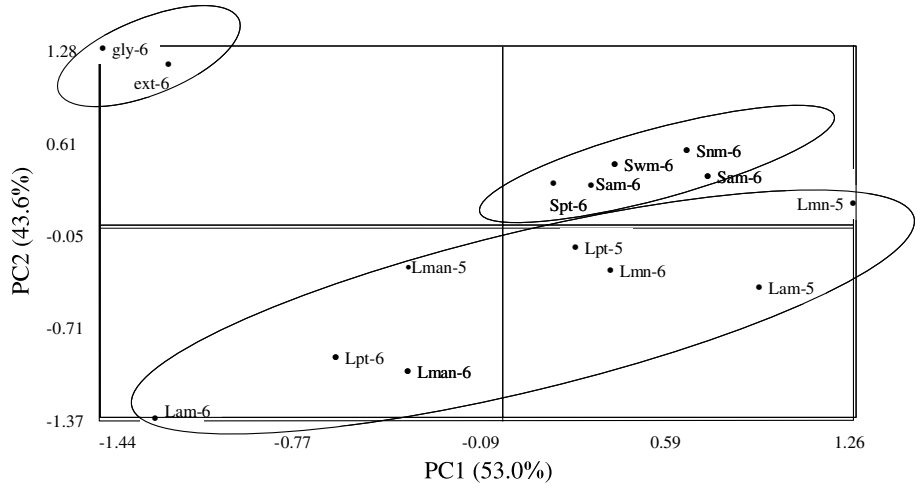

Fig. 6. PCA plot of the FTIR spectra for the samples above 15–21% w/w db. Names appear as following L: lintner; S: granular starch; ext: extrudate; gly: glycogen; pt: potato; man: manioc; am: high-amylose maize; nm: normal maize; wm: waxy maize. Numbers correspond to the conditioning hygrometries: 0, 0; 1, 0.43; 2, 0.58; 3, 0.71; 4, 0.75; 5, 0.84 and 6, 0.90.

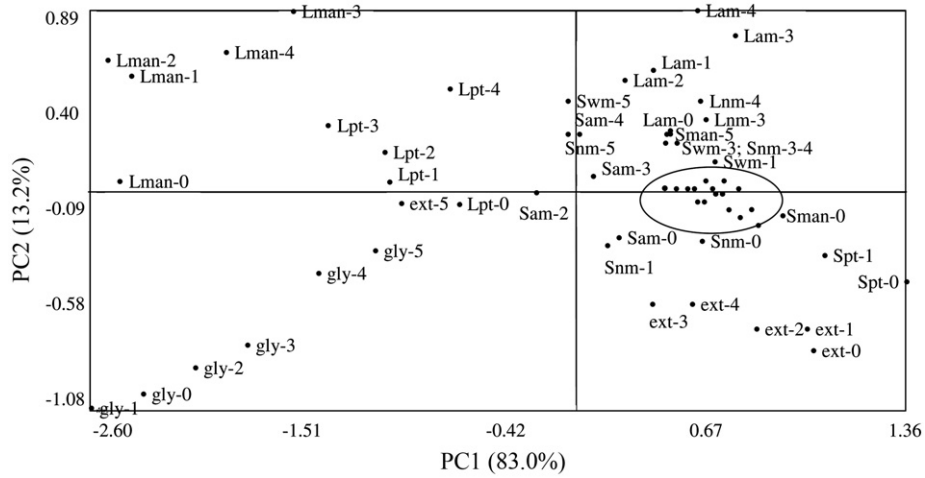

Fig. 7. PCA plot of the FTIR spectra for the samples below 15–21% w/w db. Names appear as in Fig. 6. In the circled area are found: Lnm-0, 1, 2; Spt-2, 3, 4, 5; Swm-0, 2; Snm-2, 3, 4; Sam-5; Sman-1, 2. Numbers correspond to the conditioning hygrometries: 0, 0; 1, 0.43; 2, 0.58; 3, 0.71; 4, 0.75; 5, 0.84 and 6, 0.90.

Above the glass to rubber transition, water acted as a plasticizer favoring the organization of helices. It is then interesting to study a sample in which the crystalline order is increased by annealing. The annealing of granular starch samples was thought to promote additional lengthening of double helices and the optimization of their registration within the crystalline lamellae (Genkina, Wasserman, & Yuryev, 2004; Tester & Debon, 2000) without increasing the percentage of crystallinity (Gouth & Pybus, 1971). Helicity order can then be discoupled from crystallinity order. A comparison of infrared spectra of native and annealed potato starches over 6 water contents (aw from 0.43 to 0.90), did not show clear differences (the spectra of the samples presenting the two extreme water contents are shown Fig. 9). Similar spectra were obtained whereas the annealing of potato starch was confirmed by a clear shift of the gelatinization temperature from 63.7 to 68.6 °C by DSC measurement and the conservation of the Maltese cross under polarized optical microscope was checked. Therefore it was shown that the elongation of helices observed during annealing remained negligible compared with the alignment due to the glass transition.

3.3. Analysis with the ratio 1000/1022 cm^{-1}

The principal component analysis showed that in this water content range, for 11 samples varying in structure, crystalline type, amylose content and botanical origin (Table 1), the main intensity variations are observed at two wavenumbers: 1000 and 1022 cm^{-1}. Rather than comparing PCA values, the absorbance ratio 1000/1022 cm^{-1} was used to compare the samples vs their individual water content. The ratio calculated for potato starch and derivate samples prepared at the different water contents (Fig. 10)

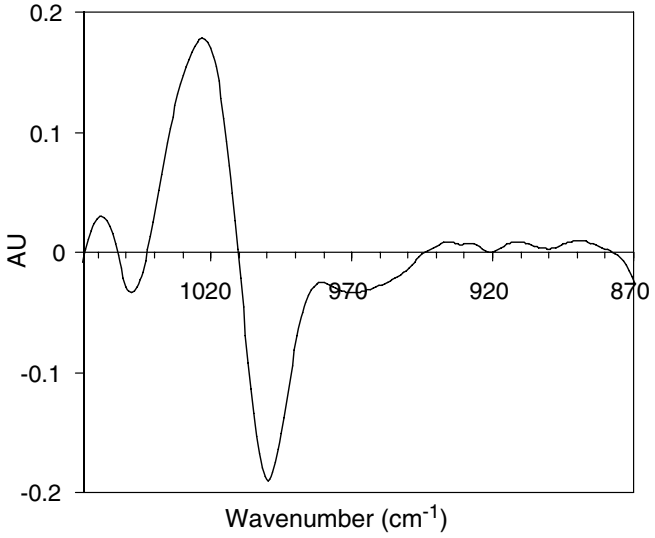

Fig. 8. Spectral pattern representing the second loading vectors determined by PCA applied to the FTIR spectra.

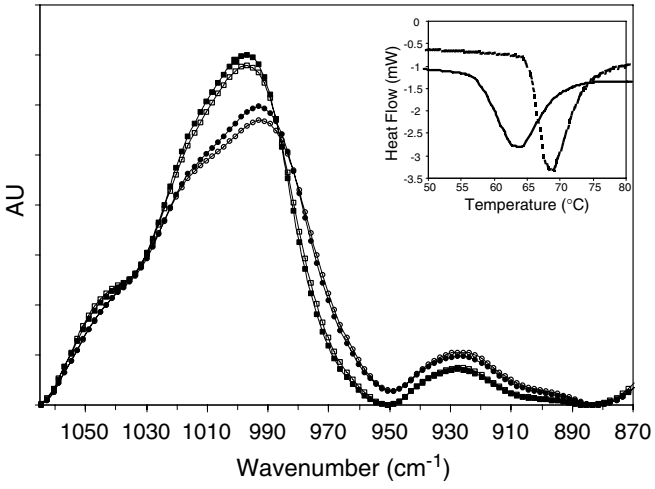

Fig. 9. FTIR spectra for granular potato starch before and after annealing hydrated over K_2CO_3: ■ native starch (14.5%); □ annealed starch (13.2%); and over $BaCL_2$ ● native starch (23.7%); ○ annealed starch (23.5%). DSC endotherms of potato starch before and after annealing is also included.

showed significant differences depending on the structure of starch (amorphous, semi crystalline, crystalline). The differences were more pronounced at high water contents (17–25% w/w db). In the particular case of the extruded sample, the peak broadening observed around 950–990 cm^{-1} with decreasing water content (Fig. 5) was accompanied by an intensity decrease at about 1000 and 1022 cm^{-1} simultaneously. Therefore no change in the intensity ratio 1000/1022 cm^{-1} was observed with varying water content (1.2 ± 0.1) suggesting an absence of structural order at the FTIR observation range. On the contrary, for lintners, a clear increase of the intensity ratio from 1.5 in anhydrous conditions (below 15% w/w db) to 2.6 at the higher hydration levels (above 15% w/w db) revealed a more ordered

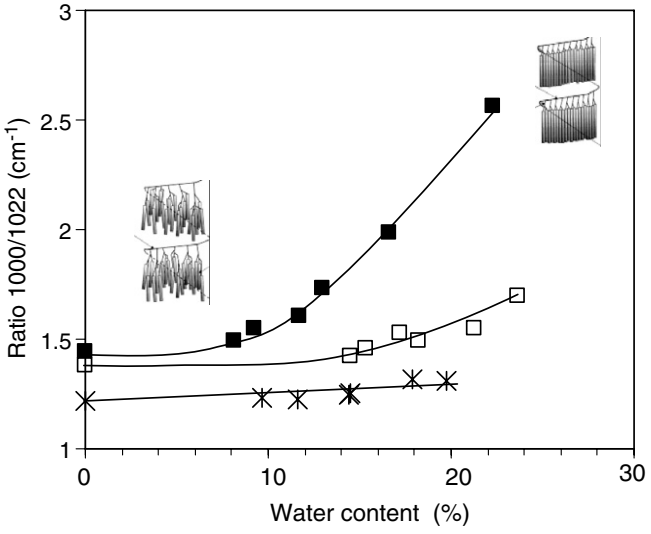

Fig. 10. IR ratio of the absorbances 1000/1022 cm^{-1} for samples derived from potato starch in three structural states with water content (the lines are only present to guide the eye). ∗ extruded starch; □ granular starch; ■ lintner (water content in w/w db).

structure. In lintners, most of the amorphous areas of granular starch have been hydrolyzed and mainly the crystalline parts remain with a part of the spacers. These samples are thereby made up of clusters of helices linked by short chains. As no variation of the 1000/1022 cm^{-1} ratio was observed for amorphous samples with the water content, it confirms that the variations observed are due to helices organization.

Similar results were obtained for manioc, maize and glycogen samples (Figs. 11 and 12). As expected, the amorphous glycogen gave similar results to those obtained with the extruded potato starch sample (1.2 ± 0.1) and was quite unmodified with the water content (0–25% w/w db). Semi-crystalline granular samples gave intermediate

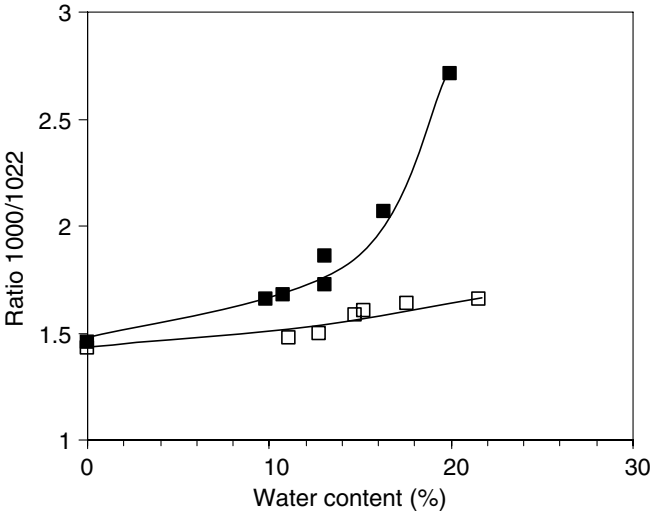

Fig. 11. IR ratio of the absorbances 1000/1022 cm^{-1} for the manioc starch and lintner vs water content (w/w db). □ granular starch; ■ lintner.

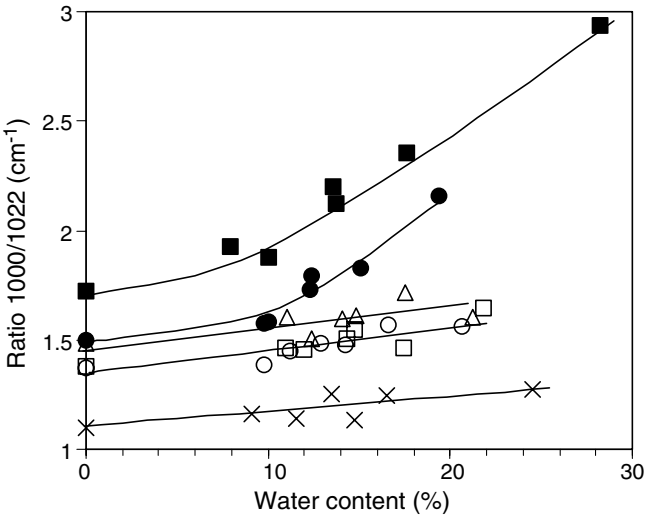

Fig. 12. IR ratio of the absorbances 1000/1022 cm^{-1} for granular starches (empty symbols) and lintners (filled symbols) vs water content (w/w db). × glycogen; □■ amylose-rich maize; ○● normal maize and △ waxy maize.

ratio values (1.4–1.7). Lintners always gave higher values (1.5–3.0) and showed steeper slopes with water content above the T_g. These results should reflect the amount of helices and the way the water molecules are distributed between the helices. On the whole, the 1000/1022 cm^{-1} ratios increased with hydrated crystalline samples (17–25% w/w db).

Although normal and high-amylose granular maize starches were composed of 25% and 70% amylose and corresponded to A and B crystalline allomorphs respectively, no difference was obtained for the 1000/1022 cm^{-1} ratios whatever the water content. Moreover, the 1000/1022 cm^{-1} ratio values for the normal potato starch composed of 20% amylose and presenting B type crystals can also superimpose on the same curve. This implies that the same helix interactions are observed whatever the amount of amylose and the crystalline type. A previous study indicated that infrared spectroscopy did not allow the characterization of long range order such as crystalline unit cells and thereby the nature of the allomorph (Sevenou et al., 2002). The change of the 1000/1022 cm^{-1} ratio was then assigned to characterize the alignment of helices at short order range.

For all samples analyzed (potato, manioc, maize), for anhydrous granular starch samples, the 1000/1022 cm^{-1} values were low and rather close (1.4 ± 0.1), whatever the intrinsic features of the starch (Table 1) showing similar glassy systems. With increasing water contents, double helices (the mesogens units) aligned promoting the formation of layered crystalline regions as revealed by X-ray measurements (Waigh et al., 1997). The use of FTIR to evidence phase transition process has already been shown for poly(phenylene sulfide) vs temperature (D'Ilario et al., 1997). This was also shown for pure 4-chloro-2′-hydroxy-4′-pentyloxyazobenzene (Czarnik-Matusewicz et al., 2005) for which a more drastic phase transition was obtained for solid/smectic phase transition whereas smectic/nematic transition gave the smaller variations. With simple molecule such as 2-biphenyl methanol compound, fine interpretation of IR bands can lead to a first band characteristic of the crystalline fraction and a second one specific of the glass formation (Baran, Davydova, & Pietraszko, 2005). Our results obtained for lintners and granular starches above T_g extend the use of FTIR as a convenient technique to evidence glass transition occurring in biopolymer systems.

As previously demonstrated (Harrick, 1979), the penetration depth of the IR beam in ATR-FTIR system is about 2 μm which is very small in regard of the size of some starch granules and notably potato starch granules which can reach 100 μm. The organization investigated by ATR could therefore be limited to the external shell (Sevenou et al., 2002). The comparative study of internal and external structure of potato starch granules was tentatively performed using cryo-grinded samples. Granule sizes measured by granulometry, decreased from mean diameters of 45 μm (native granules) to 36 μm (cryo-grinded granules). This latter sample appeared as a mix of granules (around 45 μm) and small fragments (around 2 μm) when observed with an optical microscope. Assuming a bimodal distribution made of native granules and fragments, the mean diameter change corresponds to a ratio 55–45 expressed on a volume basis native granule/fragment, 35–65 on a surface basis. So the measured signal can be considered representative of the internal parts of the granules. The comparison of infrared spectra recorded before and after cryogrinding and at 6 humidity levels indicated that the 1000/1022 cm^{-1} ratio was unchanged and could not discriminate between the internal and external parts of potato starch granules. To confirm these results, same unchanged spectra were obtained when comparing native and cryo-grinded high-amylose maize starches at various water contents. The alignment of helices at a given water content was, therefore, supposed to be similar inside and at the surface of the granules.

3.4. Toward an infrared crystalline phase index

The ratio of absorbances 1000/1022 cm^{-1} showed more pronounced variations for samples containing more semi-crystalline domains. This ratio, corrected for the contribution of the amorphous part (as obtained for glycogen in the same conditions), was calculated for each sample conditioned at an hygrometry of 0.90 ($BaCl_2$ saturated salt). At this hygrometry, all samples are in the rubbery state.

Plotting the X-ray crystallinity index as a function of the smectic IR index for all the samples reveals a strong non linear relationship (Fig. 13). A linear relationship would have meant that X diffractometry and FTIR are measuring parallel orders. X-ray measures an order at a scale which is much larger than the one obtained by FTIR.

No order is measured for amorphous samples by any of the two techniques. In a first phase, the X-ray index

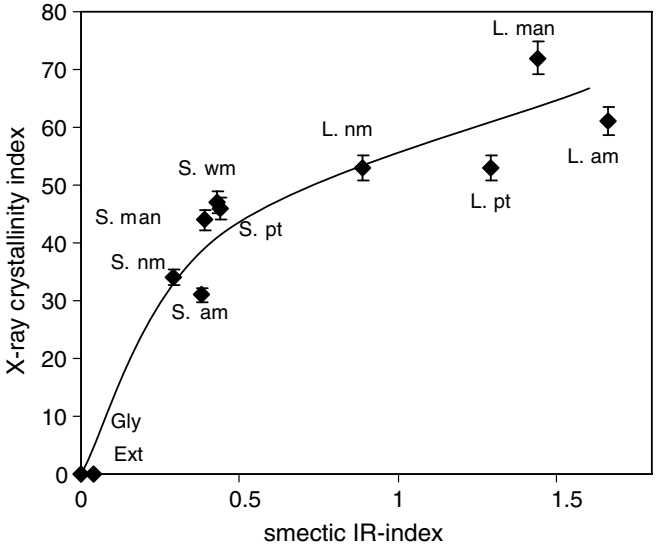

Fig. 13. Crystalline phase index as obtained by IR ratio 1000/1022 cm^{-1} corrected for the amorphous contribution (glycogen value at aw = 0.90) against% crystallinity obtained by X-ray measurements (Planchot, 1993). (Names appear as in Fig. 6.)

increases linearly to the FTIR index for native starches. In a second phase, the crystallinity X-ray index increases with a lower slope. This means that ordered zones in this second group of samples are more important when determined by FTIR than by X-ray diffractometry. This second group of samples is composed of lintners, where most of amorphous zones of semicrystalline granular starches were removed during the lintnerisation process. So a larger amount of ordered clusters in the crystalline lamellae were taken in account at the FTIR scale showing a more precise depiction of the crystalline zones compared to X-ray diffractometry. Indeed less structural defaults are considered at this scale compared to the crystal lattice X-ray range.

4. Conclusion

The infrared spectra of lintners recorded at various water contents showed an intense absorption at 1000 cm^{-1} assigned to hydrated crystalline domains whereas the band at 1022 cm^{-1} revealed the amorphous contribution. A principal component analysis carried out on 11 samples varying in structure (amorphous, semi-crystalline, crystalline), crystalline type, amylose content and botanical origin showed a major contribution of the 1000/1022 cm^{-1} ratio. Clear changes on the spectra observed below and above the glass transition induced an analysis according to double helices reorganization. The increase of the 1000/1022 cm^{-1} ratio was thought to characterize double helices reaching a more ordered structure. No change in the band at 1047 cm^{-1} was observed, which demonstrates that no formation of helices or packing of helices were induced over hydration. Also the absence of 1000/1022 cm^{-1} variation for amorphous samples confirmed that the reorganization as followed by FTIR concerned crystalline lamellae.

Under anhydrous conditions, for all samples the low 1000/1022 cm^{-1} ratio values accompanied by peak broadening were attributed to the distortion of the liquid crystal. The unorganized lamellae were forming a nematic structure. Upon hydration, the ratio increased drastically mainly for lintners, the most crystalline samples. This was interpreted as mesogenic units sliding over each others, arranging helices localized inside the crystallites, into a flat layered smectic structure. The 1000/1022 cm^{-1} ratio appeared therefore sensitive to the nematic–smectic transition according to the side-chain liquid crystalline polymer (SCLCP) model.

Ratio changes were more largely function of the water content when the helices content was high. We proposed to use this change as a measure of the relative fractions of smectic mesophases in starchy materials by comparing the values obtained on moistured samples, achieved after conditioning at 0.90 hygrometries. This study illustrates that FTIR can be a useful technique to follow phase transitions on biopolymers. Further work is in progress to assess the transition smectic–nematic – isotropic as a function of temperature.

Acknowledgements

This work was funded by the French research agency ANR (ACI NR183 BIOSYAMI). The authors are grateful to E. Perrin and J. Davy (INRA Nantes, France) for the water content and DSC measurements, respectively.

References

Baran, J., Davydova, N. A., & Pietraszko, A. (2005). Spectroscopic study of the formation of molecular glasses. *Journal of Molecular Structure, 744*, 301–305.

Bernazzani, P., Chapados, C., & Delmas, G. (2000). Double-helical network in amylose as seen by slow calorimetry and FTIR. *Journal of Polymer Science B: Polymer Physics, 38*, 1662–1677.

Bizot, H., Le Bail, P., Leroux, B., Davy, J., Roger, P., & Buléon, A. (1997). Calorimetric evaluation of the glass transition in hydrated, linear and branched polyanhydroglucose compounds. *Carbohydrate Polymers, 32*, 33–50.

Buléon, A., Colonna, P., Planchot, V., & Ball, S. (1998). Starch granules: structure and biosynthesis. *International Journal of Biological Macromolecules, 23*, 85–112.

Buléon, A., Gérard, C., Riekel, C., Vuong, R., & Chanzy, H. (1998). Details of the crystalline ultrastructure of C-starch granules revealed by synchrotron microfocus mapping. *Macromolecules, 31*, 6605–6610.

Cael, J. J., Koenig, J. L., & Blackwell, J. (1973). Infrared and Raman spectroscopy of carbohydrates. Part III: Raman spectra of the polymorphic forms of amylose. *Carbohydrate Research, 29*, 123–134.

Cael, J. J., Koenig, J. L., & Blackwell, J. (1975). Infrared and Raman spectroscopy of carbohydrates. Part IV: Normal coordinate analysis of V-amylose. *Biopolymers, 14*, 1885–1903.

Cameron, R. E., & Donald, A. M. (1993). A small-angle X-ray scattering study of the absorption of water into the starch granule. *Carbohydate Research, 244*, 225–236.

Czarnik-Matusewicz, B., Pajak, J., & Rospenk, M. (2005). The phase transition temperatures of a liquid crystal determined from FT-IR

spectra explored by principal component analysis. *Spectrochimica Acta Part A, 62*, 157–163.

Daniels, D. R., & Donald, A. M. (2004). Soft material characterization of the lamellar properties of starch: smectic side-chain liquid-crystalline polymeric approach. *Macromolecules, 37*, 1312–1318.

Della Valle, G., Boche, Y., Colonna, P., & Vergnes, B. (1995). The extrusion behaviour of potato starch. *Carbohydrate Polymers, 28*, 255–264.

D'Ilario, L., Lucarini, M., Martellini, A., & Piozzi, A. (1997). Poly(*p*-phenylene sulfide) glass transition temperature evidences by IR spectroscopy. *European Polymer Journal, 33*, 1809–1811.

French, D. (1984). Organization of starch granules. In R. L. Whistler, J. N. BeMiller, & E. F. Paschall (Eds.), *Starch: chemistry and technology* (2nd ed., pp. 183–247). London: Academic Press.

Genkina, N. K., Wasserman, L. A., & Yuryev, V. P. (2004). Annealing of starches from potato tubers grown at different environmental temperatures. Effect of heating duration. *Carbohydrate Polymers, 56*, 367–370.

Goodfellow, B. J., & Wilson, R. H. (1990). A Fourier transform IR study of the gelation of amylose and amylopectin. *Biopolymers, 30*, 1183–1189.

Gouth, B. M., & Pybus, J. N. (1971). Effect on the gelatinization temperature of wheat starch granules of prolonged treatment with water at 50 °C. *Starch, 23*, 210–212.

Guilbot, A., & Mercier, C. (1985). The polysaccharides. In: G. O. Aspinall, Vol. 3 (pp. 209–282). London: Academic Press.

Harrick, N. J. (1979). *Internal reflection spectroscopy. Harrick Scientific Corporation*. New York: Wiley.

Imberty, A., Buléon, A., Tran, V., & Perez, S. (1991). Recent advances in knowledge of starch structure. *Starch, 43*, 375–384.

Imberty, A., Chanzy, S., Perez, S., Buléon, A., & Tran, V. (1988). The double-helical nature of the crystalline part of A-starch. *Journal of molecular biology, 201*, 365–378.

Kacurakova, M., & Mathlouthi, M. (1996). FTIR and laser-raman spectra of oligosaccharides in water: Characterization of the glycosidic bond. *Carbohydrate Research, 284*, 145–157.

Liu, Q., Charlet, G., Yelle, S., & Arul, J. (2002). Phase transition in potato starch-water system I. Starch gelatinization at high moisture level. *Food Research International, 35*, 397–407.

Liu, Y., Himmelsbach, D. S., & Barton, F. E. (2004). Two-dimensional Fourier transform Raman correlation spectroscopy determination of the glycosidic linkages in amylose and amylopectin. *Applied Spectroscopy, 58*, 745–749.

Maréchal, Y., & Chanzy, H. (2000). The hydrogen bond network in Iβ cellulose as observed by infrared spectroscopy. *Journal of molecular structure, 523*, 183–196.

McKenna, L., Miller, L. S., & Peterson, I. R. (2004). Polymer dispersed liquid crystal films for modulating infra-red radiation. *Polymer, 45*, 6977–6984.

Nair, R., Nyamweya, N., Gonen, S., Martinez-Miranda, L. J., & Haog, S. W. (2001). Influence of various drugs on the glass transition temperature of poly(vinylpyrrolidone): a thermodynamic and spectroscopic investigation. *International Journal of Pharmaceutics, 225*(1–2), 83–96.

Nayouf, M., Loisel, C., & Doublier, J.-L. (2003). Effect of thermomechanical treatment on the rheological properties of crosslinked waxy corn starch. *Journal of Food Engineering, 59*, 209–219.

Oostergetel, G. T., & van Bruggen, E. F. J. (1993). The crystalline domains in potato starch granules are arranged in a helical fashion. *Carbohydrate Polymers, 21*, 7–12.

Paris, M., Bizot, H., Emery, J., Buzaré, J. Y., & Buléon, A. (1999). Crystallinity and structuring role of water in native and recrystallized starches by ^{13}C CP-MAS NMR spectroscopy 1: spectral decomposition. *Carbohydrate Polymers, 39*, 327–339.

Planchot, V., PhD thesis 1993. α-amylases d'Aspergillus fumigatus: mécanismes d'action en phase hétérogène. University of Nantes.

Robert, P., Devaux, M.-F., & Bertrand, D. (1996). Beyond prediction : extracting relevant information from near infrared spectra. *Near Infrared Spectroscopy, 4*, 75–84.

Robin, J. P., Mercier, C., Duprat, F., Charbonnière, R., & Guilbot, A. . *Die Starke, 27*, 36–45.

Sevenou, O., Hill, S. E., Farhat, I. A., & Mitchell, J. R. (2002). Organisation of the external region of the starch granule as determined by infrared spectroscopy. *International Journal of Biological Macromolecules, 31*, 79–85.

Slade, L., & Levine, H. (1993). Water relationships in starch transitions. *Carbohydrate Polymers, 21*, 105–131.

Tester, R. F., & Debon, S. J. J. (2000). Annealing of starch – a review. *International Journal of Biological Macromolecules, 27*, 1–12.

van Soest, J. J. G., Tournois, H., de Wit, D., & Vliegenthart, J. F. G. (1995). Short-range structure in (partially) crystalline potato starch determined with attenuated total reflectance Fourier-transform IR spectroscopy. *Carbohydrate Research, 279*, 201–214.

Vasco, P. D., Blackwell, J., & Koenig, J. L. (1971). Infrared and Raman spectroscopy of carbohydrates. Part I: Identification of O–H and C–H related vibrational modes for D-glucose, maltose, cellobiose, and dextran by deuterium-substitution methods. *Carbohydrate Research, 19*, 297–310.

Vasco, P. D., Blackwell, J., & Koenig, J. L. (1972). Infrared and Raman spectroscopy of carbohydrates. Part II: Normal coordinate analysis of α-D-glucose. *Carbohydrate Research, 23*, 407–416.

Waigh, T. A., Hopkinson, I., Donald, A. M., Butler, M. F., Heidelbach, F., & Riekel, C. (1997). Analysis of the native structure of starch granules with X-ray microfocus diffraction. *Macromolecules, 30*, 3813–3820.

Waigh, T. A., Kato, K. L., Donald, A. M., Gidley, M. J., Clarke, C. J., & Riekel, C. (2000). Side-chain liquid-crystalline model for starch. *Starch, 52*, 450–460.

Wilson, R. H., Kalichevsky, M. T., Ring, S. G., & Belton, P. S. (1987). A Fourier-transform infrared study of the gelation and retrogradation of waxy-maize starch. *Carbohydrate Research, 166*, 162–165.

Wolkers, W. F., Oliver, A. E., Tablin, F., & Crowe, J. H. (2004). A Fourier-transform infrared spectroscopy study of sugar glasses. *Carbohydrate Research, 339*, 1077–1085.